*Int. J. Electrochem. Sci.*, 15 **(2020)** 4494 – 4502, doi: 10.20964/2020.05.33

International Journal of
ELECTROCHEMICAL
SCIENCE
www.electrochemsci.org

# Up-scalable synthesis of highly crystalline electroactive Ni-Co LDH nanosheets for supercapacitor applications

*G.E. Nyongombe*[1], *G.L. Kabongo*[1,2,3,*], *L.L. Noto*[1], *M.S. Dhlamini*[1,*]

[1] Department of Physics, School of Science, CSET, University of South Africa, Private Bag X6, Florida, 1710, Science Campus, Christiaan de Wet and Pioneer Avenue, Florida Park, Johannesburg, South Africa
[2] TS&BHP S.E.N.C., Saint-Jean-sur-Richelieu, Québec J3B 6X4, Canada
[3] Département de Physique, FNEA, Université Pédagogique Nationale, 8815 Kinshasa, R.D. Congo
[*]E-mail: leba.kabongo@gmail.com, dhlamms@unisa.ac.za

*Received:* 5 August 2019 / *Accepted:* 22 September 2019 / *Published:* 10 April 2020

The development of cost-effective and scalable synthetic methods is of paramount importance to achieve industrial application of energy conversion and storage devices based on layered double hydroxides (LDH). Herein, we synthesized NiCo-LDH nanosheets via a simple up-scalable co-precipitation method at relatively low temperature. Moreover, we used several characterization techniques to unveil the unique properties of the novel NiCo-LDH among which XRD, EDS, XPS and FT-IR. Consequently, we further investigated NiCo-LDH nanosheets using cyclic voltammetry (CV) and electrochemical impedance spectroscopy (EIS) to evaluate the electroactivity of the as-synthesized NiCo-LDH for energy storage. Overall, the electrochemical test of the as-synthesized NiCo-LDH revealed remarkable performance exhibiting a specific capacitance as high as 2,140 $Fg^{-1}$ (5 mV/s).

**Keywords**: NiCo-LDH nanosheets, co-precipitation, EIS, cyclic voltammetry, supercapacitor

## 1. INTRODUCTION

Over the past two decades, scientists in the global technological arena have conducted gigantic research and development initiatives to practically develop energy storage devices [1-4]. Layered double hydroxides (LDH) a class of ionic lamellar compounds, also known as anionic clays have tremendously attracted scientific attention worldwide. Accordingly, they became the center of a massive technological interest because of their excellent properties such as facile synthesis, unique structure, unvarying distribution of diverse metal cations in the brucite layer, surface hydroxyl groups, easy tunability, intercalated anions with interlayer spaces, good chemical stability and the ability to intercalate diverse varieties of anions (inorganic, organic, biomolecules, and even genes) [5]. The

unique advantages of LDH among others layered materials are the possibility to obtain through the synthesis the compositions and the combinations of metal-anions [5].

Several authors have reported studies related to the synthesis of Layered Double Hydroxides (LDH). Thus, various simple as well as expensive ways to synthesize Layered Double Hydroxides (LDH) for various applications were discussed [6-8]. However, previous studies on LDH were mostly focused on the controlled morphology, the enhanced surface area and other significant properties [9-12]. Nevertheless, the astonishing scarcity of studies focusing on large scale synthesis of LDH open doors to the greatest possible progress in the field for practical applications highly needed [13].

In this present study, we have successfully synthesized and presented the facile and scalable methodology to synthesize a novel NiCo-LDH nanosheets material having a high cristallinity and exhibiting good electrochemical properties for supercapacitor electrode applications relative to previous studies [13].

## 2. EXPERIMENTAL

### *2.1. Synthesis of NiCo-LDH nanosheets*

The as-synthesized NiCo-LDH nanosheets were synthesized via co-precipitation method (Fig. 1a). All the chemicals purchased from Sigma-Aldrich was used without further purification. In a typical procedure, 10 mmol of $Ni(NO_3)_2 \bullet 6H_2O$ and 20 mmol of $Co(NO_3)_2 \bullet 6H_2O$ were dispersed in an initial solution containing 152 ml of $(CH_2OH)_2$ in 60 ml of deionized water under vigorous stirring for 8 minutes. Thereafter, 148 mmol of Urea were added to the mixture solution while maintaining vigorous stirring for another 12 minutes. The final solution was further aged for 3 h at 90°C. Finally, the precipitates were filtered and washed with deionized water and ethanol several times and dried at 80°C overnight. The as-obtained product was named NiCo-LDH@80°C having (Ni:Co=1/2) atomic ratio.

### *2.2. Materials characterization and electrochemical measurements*

XRD study was conducted using a RigakuSmartlab diffractometer ($\lambda$ = 1.54 nm). FT-IR spectrum was recorded using IR Tracer-100-SHIMADZU (3750-500 $cm^{-1}$). The morphology and chemical composition of the sample were characterized by scanning electron microscope (SEM-EDS JEOL JSM-7800F) coupled to EDS detector. XPS measurements were conducted using a KRATOS-SUPRA spectrometer using a monochromatic Al Kα radiation with hν=1486.6 eV and a base pressure of $1.2*10^{-8}$Torr.

The slurry was prepared by blending the active material, carbon black and polyvinylidene fluoride (PVDF) in a ratio of (80:10:10) in N-methylpyrrolidone (NMP) and sonicated for 10 min. The obtained slurry (100 μL) was drop-cast on glassy carbon and allowed to dry. Electrochemical data were collected on an Autolab PGSTAT302N potentiostat using a three-electrode system. Glassy carbon, platinum wire and Ag/AgCl (3 M KCl-filled) were used as working, counter and a reference

electrode, respectively. 1 M $Na_2SO_4$ solution was used as electrolyte. Finally, EIS measurements were performed with AC amplitude of 5 mV in the frequency range of 100 kHz-100 mHz.

## 3. RESULTS AND DISCUSSION

XRD and FTIR served to conduct structural studies of NiCo-LDH@80°C sample (Fig. 1). As depicted in Fig. 1b the diffraction peaks centered at 12.28°, 24.67°, 33°, 36.41° and 59° were attributed to (003), (006), (009), (012) and (110) plane of hydrotalcite-structure (JCPDS # 14-0191) standard card, respectively [14]. Moreover, the crystallinity of the as-synthesized sample as demonstrated via XRD patterns confirms the reliability of the adopted synthesis method to produce highly crystalline NiCo-LDH nanosheets.

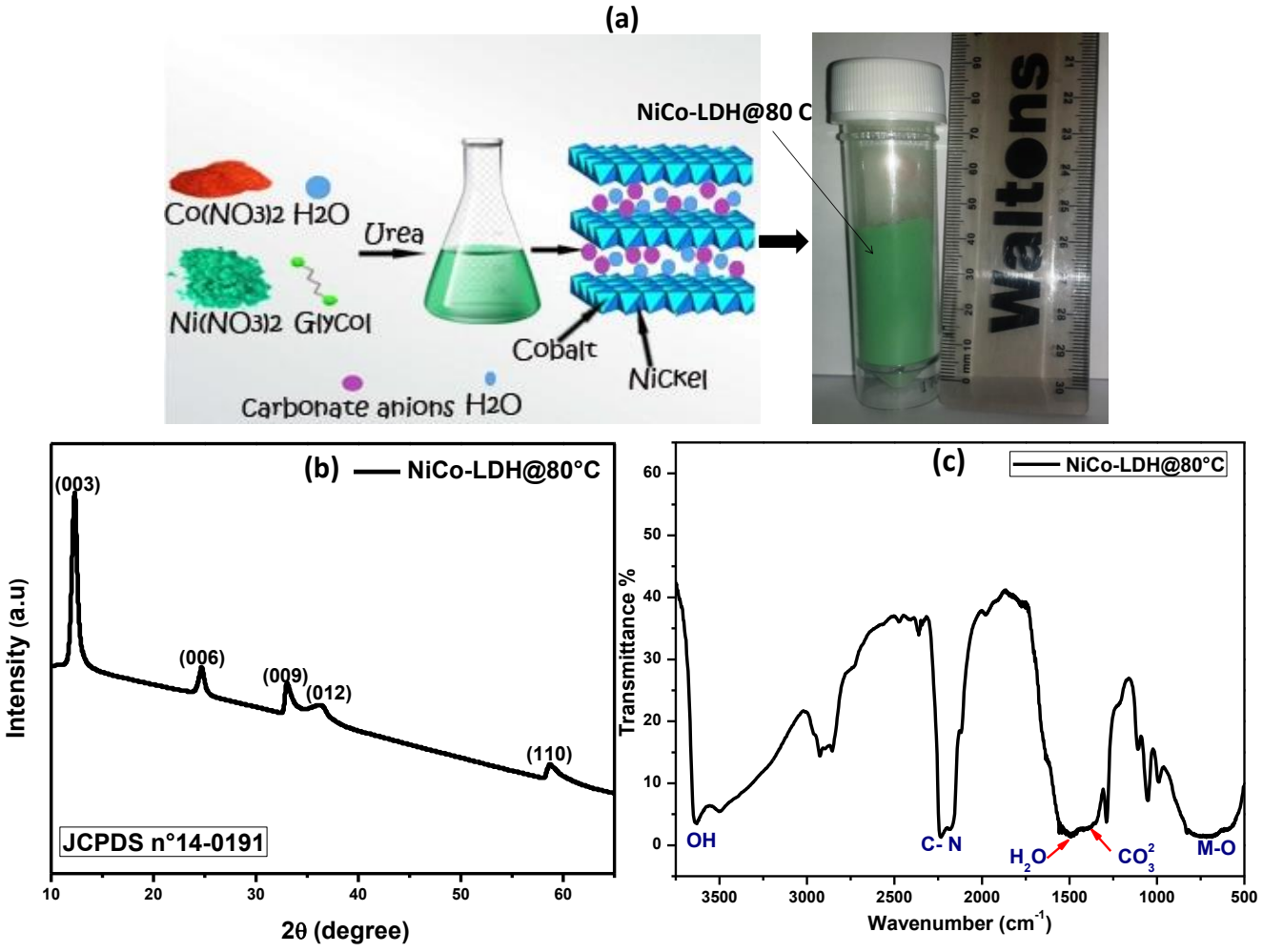


**Figure 1**. (a) Synthesis route, (b) XRD patterns and (c) FTIR spectrum of NiCo-LDH@80°C.

**Fig. 1c** displays the FTIR spectrum of NiCo-LDH@80°C which exhibited a broad peak around 3635 $cm^{-1}$ assigned to O-H stretching vibrations related to water molecules and OH groups at the brucite-like layer and interlayer, following by a peak at 1500 $cm^{-1}$ [8]. However, the peak at 1388 $cm^{-1}$

can be assigned to the vibration stretching of interlayer carbonate anions retained in the interlayer of LDH, while the peak at 638 $cm^{-1}$ was ascribed to metal-oxygen (M-O) stretching and bending vibrations in the brucite-like lattice, confirming the existence of Nickel and Cobalt in the composite [13]. In addition, the peak located at 2241 $cm^{-1}$ was assigned to the stretching vibrations of C≡N functional group.

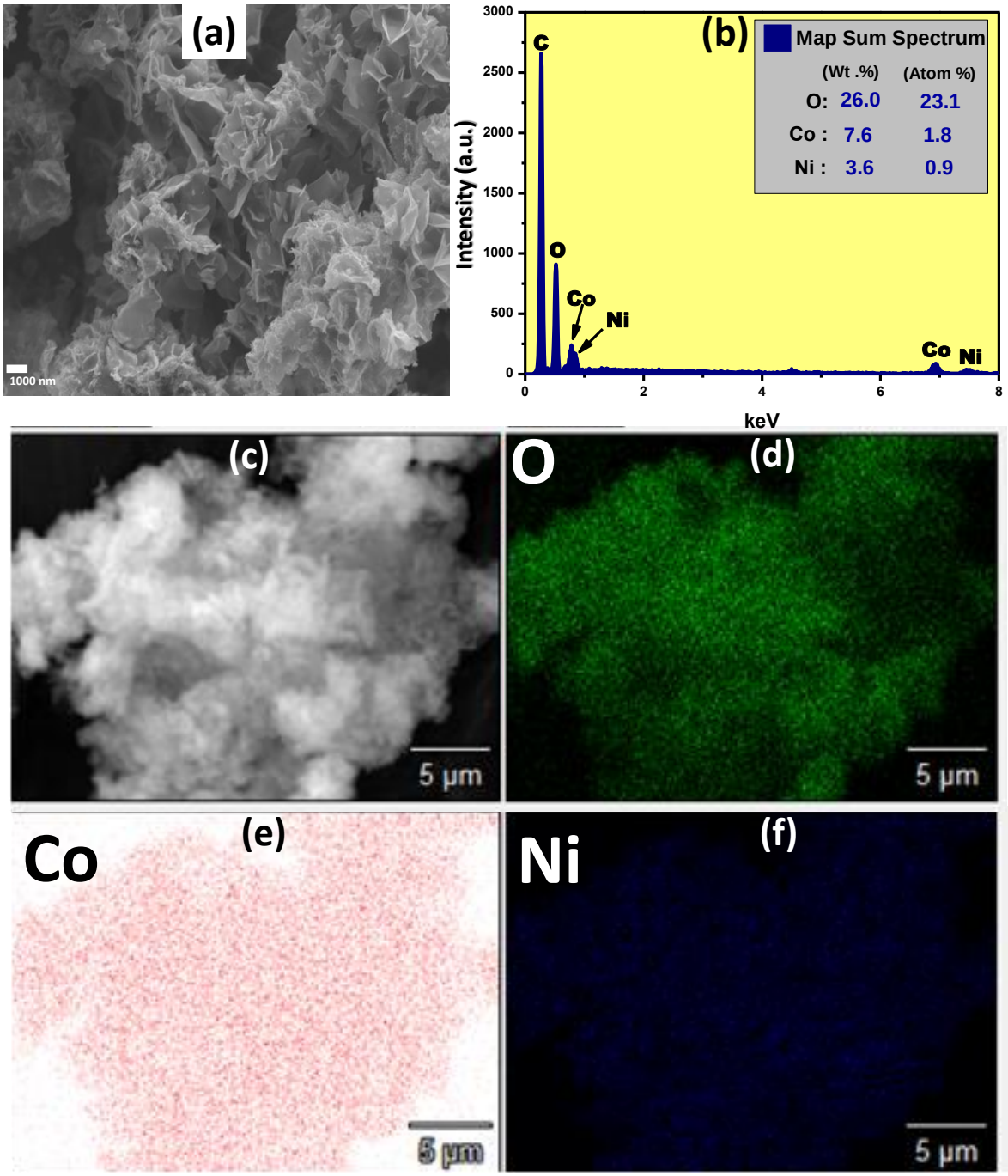


**Figure 2**. (a) FE-SEM micrograph and (b) EDS spectrum of NiCo-LDH@80°C. (c) FE-SEM image of the area used to conduct EDS mappings and (d-f) corresponding elemental mappings of O, Co and Ni.

The morphology of NiCo-LDH@80°C was characterized using SEM (Fig. 2a) which exhibited a good arrangement of nanosheets linked each other and presenting a structure like flowers. Moreover, Fig. 2b depicts the EDS spectrum of NiCo-LDH@80°C which revealed the presence of all expected chemical elements among which Nickel, Cobalt and Oxygen without impurities revealing the integrity of sample synthesis and handling. More interestingly, the distribution of all elements was relatively homogenous as revealed in Fig. 2(c-f). However, the detected carbon was due to carbon tape resulting from SEM sample preparation. Finally, it was found that the atomic ratio (Ni:Co = 1:2) was strictly in accordance with the initial weights.

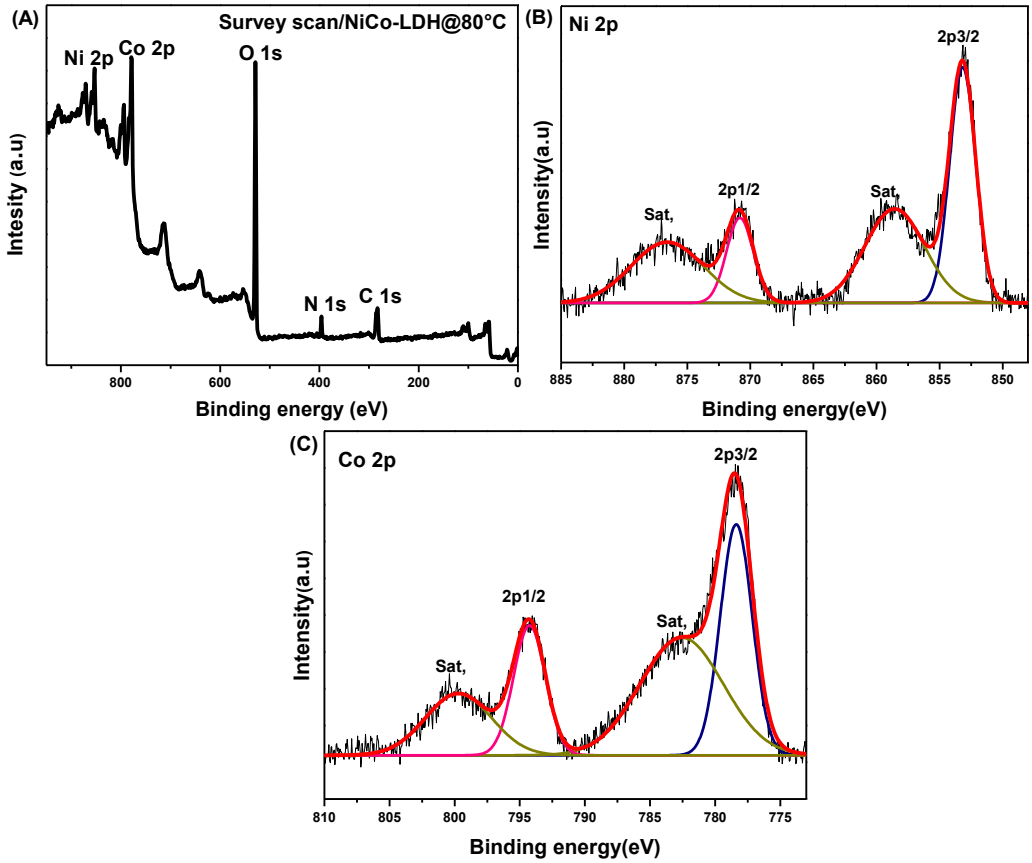


**Figure 3**. (a) XPS survey scan, HRXPS spectra of (b) Ni 2p and (c) Co 2p core-levels for NiCo-LDH@80°C.

To further investigate the surface composition and valence states XPS survey scan spectrum of NiCo-LDH@80°C (Fig. 3a) clearly demonstrated the coexistence of all expected elements which were Ni, Co and O. The XPS results are in accordance with the former EDS results presented and discussed above. On the other hand, high resolution XPS spectra were collected to get more insight on the valence states of elements on the surface. High resolution spectra of NiCo-LDH@80°C revealed that both Ni 2p and Co 2p were split into doublets due to spin-orbit splitting (Fig.3b and c) [9]. Fig. 3b presents Ni 2p core-level doublet showing a lower binding energy component Ni $2p_{3/2}$ at 853 eV and a well-defined satellite peak 858 eV of the binding energy (BE). The main peak located at 853 eV was

ascribed to metallic Ni which corresponds to $Ni^{2+}$ due to the surface oxidation confirming that $Ni^{2+}$ was present in the hydroxide material. Similarly, the Peak at 870 eV and 876 eV were assigned to Ni $2p_{1/2}$ and satellite, respectively [15, 16]. On the other hand, Fig. 3c displays Co 2p core-level spectrum of NiCo-LDH@80°C. As previously described for Ni 2p core-level Co 2p appeared as a doublet exhibiting peaks at 794 eV and 779 eV respectively assigned to Co $2p_{1/2}$ and $2p_{3/2}$ [17]. Finally, it is worth mentioning that the satellite peak observed at 784 eV is in accordance with the BE of $Co^{2+}$ [9].

Electrochemical measurements were conducted to unveil the electrochemical performances of NiCo-LDH@80°C sample which was evaluated using a standard three-electrode system in 1 M $Na_2SO_4$ electrolytic solution. Fig. 4a shows the CV curves of NiCo-LDH@80°C at (5, 10, 20, 30 50, 75 and 100 mV/s). Surprisingly, the curves show nearly a symmetrical rectangular shape in the voltage window of 0.2-0.6 V, indicating the best capacitive behavior of as-synthesized NiCo-LDH@80°C. Consecutively, the overall capacitance was due to the dual contribution of both double-layer capacitance and pseudocapacitance. It is worth mentioning that the pseudocapacitive behavior observed in the scan range of 0.3 V-0.5 V could be attributed to the faradic redox reaction occurring between M-OH and M-O-O-H (with M representing the Ni or Co ions) [18]. Additionally, it should be pointed out that no inherent shape change due to the variation of the scan rate from 5 mV/s up to 100 mV/s was noticed, indicating high-rate performance and relatively high-current capability [19,20]. Interestingly, unlike $Na_2SO_4$ electrolyte the pseudocapacitive behavior was found to be much more pronounced for KOH electrolyte as shown in the cyclic voltammetry curves in Fig. 4c. To further quantify the electrochemical behavior of NiCo-LDH@80°C, the galvanostatic Charge/Discharge curves are displayed in Fig. 4b. The linear shape of the GCD curves indicates the ideal EDLC behavior of NiCo-LDH@80°C corresponding to the nearly rectangular shape observed in the CV profile. It is worth mentioning that the symmetric GCD curves reveal the high reversible characteristic of the reactions that occur at the electrode/electrolyte interface. Finally, the electrochemical investigation in KOH electrolyte revealed that NiCo-LDH@80°C exhibited a remarkably high pseudocapacitive behavior. This finding is in accordance with previous reports [9,21].

The specific capacitance ($C_{sp}$) of NiCo-LDH@80°C was calculated from CV curves using the equation (1) below and a record high specific capacitance of 2,140 $F.g^{-1}$ obtained at 5 mV/s.

$$C_{sp} = \frac{\int_{E_1}^{E_2} i(E)dE}{2(E_2 - E_1)\ mV} \quad (1)$$

Where $C_{sp}$ is the specific capacitance ($F.g^{-1}$), $\int_{E_1}^{E_2} i(E)dE$ is total voltammetric charge which is the result of the integration of positive and negative sweep in the cyclic voltammogram. ($E_2$-$E_1$) is the potential window (V) of operation, *m* is the mass (g) of the active material after deposition of slurry and *V* is the scan rate (V/s) [22]. Interestingly, compared to previous reports available in the literature on NiCo-LDH supercapacitor electrode materials, our NiCo-LDH system exhibited higher specific capacitance than 79 % of them as illustrated in Table 1.

As depicted in Fig. 3d, electrochemical impedance spectroscopy (EIS) was carried out to further investigate the electrochemical properties of NiCo-LDH@80°C with Nyquist plot recorded in the range of 100 kHz to 100 mHz at the open circuit potentials. Ordinarily, the vertical slope in the

lower frequency range of the plot indicates low ionic diffusion resistance and charge transfer at the interface between NiCo-LDH@80°C electrode and electrolyte [23]. Finally, the slight semicircle is the result of a relatively low interfacial resistance in the system.

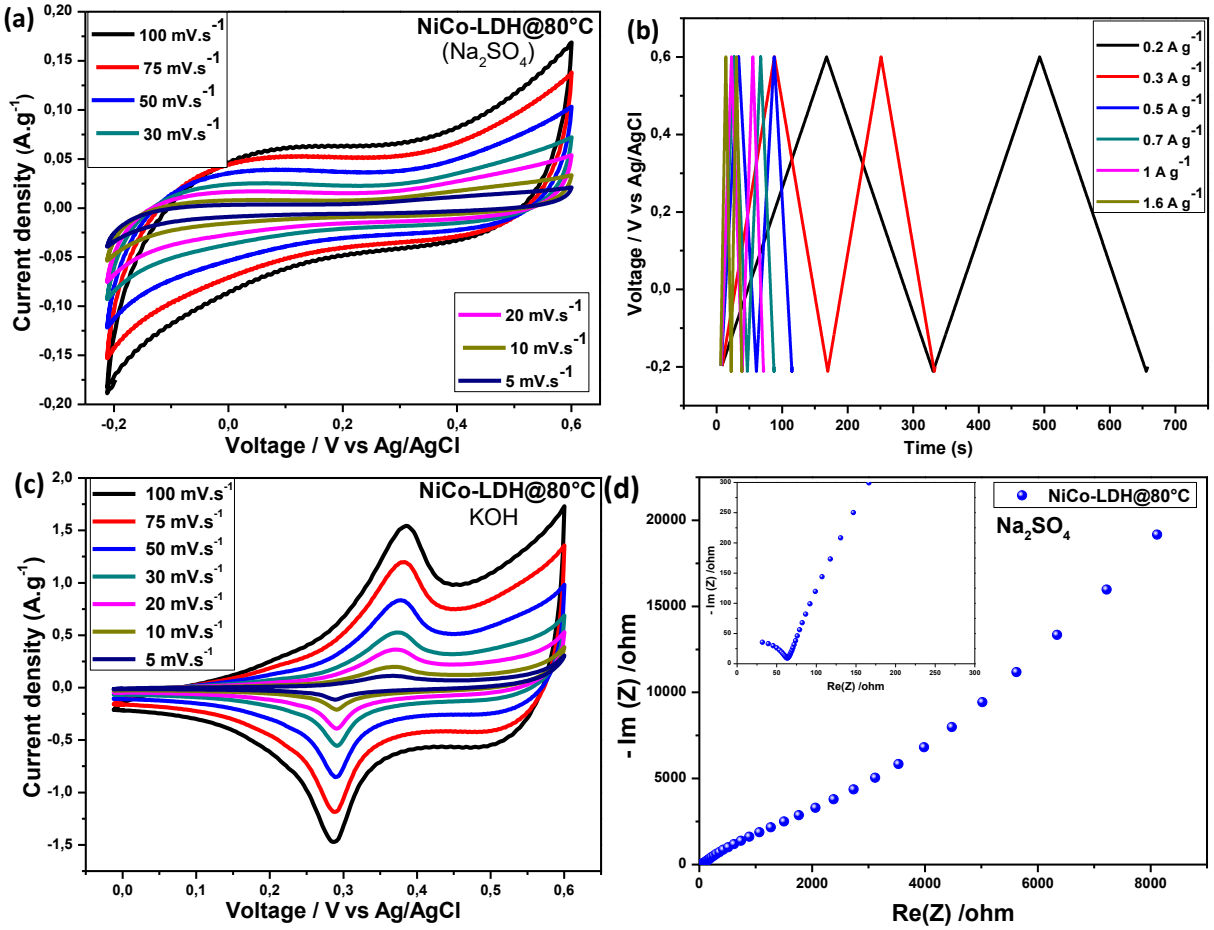


**Figure 4**. (a) CV curves of NiCo-LDH@80°C with various scan rates in 1 M $Na_2SO_4$ and (b) corresponding GCD at different current density; (d) Nyquist plots of NiCo-LDH@80°C and (c) CV profiles of NiCo-LDH@80°C 1 M KOH electrolyte.

**Table 1.** Specific capacitance performance of various NiCo-LDH based electrode.

| Active material | Configuration | electrolyte | Specific Capacitance | References |
|---|---|---|---|---|
| (Ni,Co)Se2/NiCo-LDH//PC | 2 electrode | 3 M KOH | 1224 F g-1 | (24) |
| NiCoAl-LDH-NPs/CH-NWs //AC | 2 electrode | 6 M KOH | 155.0 F $g^{-1}$ (1.0 A $g^{-1}$) | (25) |
| NiCo LDH nanoarrays | 3 electrode | 2M KOH | 2391 F $g^{-1}$ | (26) |
| PANI/NiCo-LDH | 3 electrode | 2 M KOH | 1845 F $g^{-1}$ (0.5 A $g^{-1}$) | (27) |
| α-phase NiCo DH microsphere | 3 electrode | 6 M KOH | 1120 F $g^{-1}$ (1 A $g^{-1}$) | (14) |
| GS/NiCo-LDH | 3 electrode | 6 M KOH | 1980.7 F g-1 ( 1 Ag-1) | (19) |

| | | | | |
|---|---|---|---|---|
| CNF@Ni-Co LDH NR/ NS | 3 electrode | - | 1378.2 F $g^{-1}$ (1 $Ag^{-1}$) | (23) |
| Ni50Co50-LDH | 3 electrode | 6 M KOH | 1537 F $g^{-1}$ (0.5 A $g^{-1}$) | (13) |
| NiCo-LDH/RGO | 3 electrode | 3 M KOH | 1911.1 F $g^{-1}$ (2 A $g^{-1}$) | (28) |
| NiCo-LDH@CNT/NF | 3 electrode | 1 M KOH | 2040 F $g^{-1}$ (1 A $g^{-1}$) | (18) |
| NiCo-LDH/CFC | 3 electrode | KOH-PVA (solid) | 2762.7 F g-1 | (9) |
| NiCo-LDH/Ag/NF hybrid | 3 electrode | 1 MKOH | 2920 $Fg^{-1}$ (5 $Ag^{-1}$) | (29) |
| $MnO_2$@NiCo-LDH/$CoS_2$ nanocages | 3 electrode | 2 M KOH | 1547 F $g^{-1}$ (1 A g-1) | (30) |
| CoNiFe-LDH/CNFs | 3 electrode | 6 M KOH | 1203 F $g^{-1}$ (1 A $g^{-1}$) | (31) |
| NiCo-LDH nanosheets | 3 electrode | 1 M $Na_2SO_4$ | 2140 F $g^{-1}$ | This work |

## 4. CONCLUSION

In summary, we successfully synthesized NiCo-LDH@80°C nanosheets via a facile up-scalable co-precipitation method. The XRD, EDS, XPS and FT-IR have confirmed the high crystallinity and stability of the as-synthesized materials. The electrochemical investigation of NiCo-LDH@80°C in 1 M $Na_2SO_4$ electrolyte resulted in a record high specific capacitance as high as 2,140 $F.g^{-1}$ (5 mV/s). Moreover, this method can be effectively up-scaled and extended to the synthesis of other LDH for various energy conversion and storage applications.

ACKNOWLEDGEMENTS
The authors are grateful to the University of South Africa (UNISA) for its generous financial support.

## References

1. M.R. Lukatskaya, S. Kota, Z. Lin, M.-Q. Zhao, N. Shpigel, M.D. Levi, J. Halim, Pierre-Louis Taberna, M.W. Barsoum, P. Simon and Y. Gogotsi, *Nat. Energy,* 2 (8) (2017) 17105.
2. X. Xu, Y. Liu, P. Dong, P.M. Ajayan, J. Shen and M. Ye, *J. Power Sources,* 400 (2018) 96.
3. O. Jung, M.L. Pegis, Z. Wang, G. Banerjee, C.T. Nemes, W.L. Hoffeditz, J.T. Hupp, C.A. Schmuttenmaer, G.W. Brudvig and J.M. Mayer, *J. Am. Chem. Soc*., 140 (11) (2018) 4079.
4. M. Li, Y. Zhu, X. Ji and S. Cheng, *Mater. Lett*., 254 (2019) 332.
5. F. Li and X. Duan, Applications of layered double hydroxides. In: Duan, X., Evans, D.G. (Eds.), Structure and Bonding. Vol.119. Springer (2006), New York, NY, USA, pp.,193–223. http://dx.doi.org/10.1007/430-007.
6. J. He, M. Wei, B. Li, Y. Kang, D.G. Evans and X. Duan, Preparation of double layered hydroxides. In: Duan, X., Evans, D.G. (Eds.), Layered Double Hydroxides. Springer (2006), Berlin, pp. 89–119.
7. S. Gamil, M.A. El Rouby Waleed, M. Antuch and I.T. Zedan, *RSC Adv*., 9 (2019) 13503.
8. V. Rives, Layered Double Hydroxides: Present and Future. Nova Science Publishers (2001) New York, NY, USA.
9. T. Wang, S. Zhang, X. Yan, M. Lyu, L. Wang, J.M. Bell and H. Wang, *ACS Appl. Mater. Interfaces,* 9(18) (2017) 15510.
10. V. Prevot, C. Forano and J.P. Besse, *Inorg. Chem*., 37 (1998) 4293.
11. G.N. Pshinko, *J. Chem*., (2013) 347178.

12. L. Qin, M. Xue, W. Wang, R. Zhu, S. Wang, J. Sun, R. Zhang and X. Sun, *Int. J. Pharm*., 388 (2010) 223–230.
13. R. Li, Z. Hu, X. Shao, P. Cheng, S. Li, W. Yu, W. Lin and D. Yuan, *Sci. Rep*., 6 (2016) 18737.
14. J. Li, M. Wei, W. Chu, and N. Wang, *Chem. Eng. J*., 316 (2017) 277.
15. H. Li, S. Lu, J. Sun, J. Pei, D. Liu, Y. Xue, J. Mao, W. Zhu and Z. Zhuang, *Chem. Eur. J.,* 24 (2018) 11748.
16. Y. Pan, Y. Liu, J. Zhao, K. Yang, J. Liang, D. Liu, W. Hu, D. Liu, Y. Liu and C. Liu, *Mater. Chem*. A, 3 (2015) 1656.
17. J.-W. Kima, S.J. Lee, P. Biswas, T.I. Lee, J.-M. Myoung, *Appl. Surf. Sci.,* 406 (2017) 192.
18. X. Li, J. Shen, W. Sun, X. Hong, R. Wang, X. Zhao and X. Yan, *J. Mater., Chem. A*, 3 (2015) 13244.
19. Y. Tao, L. Ruiyi and L. Zaijun, *Mater. Res. Bull*., 51 (2014) 97.
20. J. Yana, Z. Fan, T. Wei, W. Qian, and F. We, *Carbon,* 48 (2010) 3825.
21. Y. Wang, D. Zhou, D. Zhao, M. Hou, C. Wang and Y. Xia, *J. Electrochem. Soc*., 160 (1) (2013) A98.
22. W. Chen, Z. Fan, L. Gu, X. Bao and C. Wan, *Chem. Commun*., 46 (2010) 3905.
23. F. Lai, Y. Huang, Y.-E. Miao and T. Liu, *Electrochim. Acta,* 174 (2015) 456.
24. X. Li, H. Wu, C. Guan, A.M. Elshahawy, Y. Dong, S. J. Pennycook, and J. Wang, Small, (2018) 1803895.
25. J. Yang, C. Yu, X. Fan and J. Qiu, *Adv. Energy Mater*., (2014) 1400761.
26. W. Zou, W. Guo, X. Liu, Y. Luo, Q. Ye, X. Xu and F. Wang, *Chem. Eur. J.,* 24 (1) (2018) 1.
27. X. Ge, Y. He, T. Plachy, N. Kazantseva, P. Saha and Q. Cheng, *Nanomaterials,* 9 (2019) 527.
28. X. Cai, X. Shen, L. Ma, Z. Ji, C. Xu, A. Yuan, *Chem. Eng. J*., 268 (2015) 251.
29. T. Guan, L. Fang, L. Liu, F. Wu, Y. Lu, H. Luo, J. Hu, B. Hu, M. Zhou, *J. Alloys Compd.,*799 (2019) 521.
30. X. Wang, F. Huang, F. Rong, Pe. He, R. Que, S. P. Jiang, *J. Mater Chem. A*, 7 (2019) 12018.
31. F. Wang, S. Sun, Y. Xu, T. Wang, R. Yu & H. Li, *Sci. Rep*. 7 (2017) 4707.